Photocatalytic Properties of Zinc Selenide and Cobalt Selenide Nanocomposite

Han Yin, Kai Bao, Yi Wang, Maojuan Bai, Jun Wan*
School of Environment and Safety Engineering Qingdao University of Science and Technology Qingdao 266042, China.
wanjundz@sohu.com*

(Received on 22nd January 2021, accepted in revised form 21st October 2021)

Summary: In recent years, the environmental pollution caused by organic dyes has become more and more serious, so the removal of organic dyes has been paid more and more attention. In this work, ZnSe/CoSe was synthesized by hydrothermal method, and the activity of the composite photocatalytic materials was detected by visible light catalytic degradation of methylene blue. The nanocomposites were characterized by Scanning Electron Microscope (SEM), Transmission Electron Microscope (TEM), Energy Dispersive Spectrometer (EDS), X-ray Powder Diffraction (XRD), Ultraviolet Diffuse Reflection Spectrum (UV-Vis), Brunner−Emmet−Teller Measurements (BET), and X-ray Photoelectron Spectroscopy (XPS). The catalytic effect was the most obvious when the composite ratio was 1:7.5, with the removal rate reaching to 99.4 % of 20 mg/L MB within 120 min of visible light irradiation. Therefore, ZnSe/CoSe has a broader application prospect due to its high efficiency and low price.

Keywords: Photocatalysis, Organic dye wastewater, Hydrothermal method, Zinc selenide, Cobaltous selenide.

Introduction

Due to the water solubility of dyes, industrial wastewater severely pollutes surrounding environment and affects biological health [1]. As environmental problems become more serious, neither physical nor chemical methods can be used to treat waste water economically and effectively, so scientists are looking for more cost-effective ways to solve this problem [2]. Solar energy has become one of the most ideal ways to degrade dye wastewater because it is clean, convenient and economical. Scientists have discovered many effective photocatalysts, such as TiO_2. The photocatalytic activity is determined by the band gap and electron configuration of the material, and it is also affected by the light absorption capacity, porous structure and charge transfer characteristics of the material [3]. Only when the absorbed photons are converted into electron-hole pairs, electron-hole pairs are separated and transported, and electron structures exist on the particle surface, can the photocatalyst have strong photocatalytic efficiency, that is, high catalytic activity [4]. However, most of the existing photocatalysts have low photodegradation efficiency, difficult recovery and complex preparation process. Therefore, developing economical photocatalyst with high degradation and photodegradation rates is the primary problem that scientists need to solve.

In recent years, semiconductor material ZnSe has attracted more and more attention in the field of production and life due to its superior chemical stability [5, 6], such as wide direct band gap of 2.7 eV, large exciton binding energy of 22 meV, high transparency in the wide range of 0.5–22 μm and small exciton Bohr diameter of 9 nm, and its potential applications in light-emitting devices [7], photo detectors [8], solar cells [9] and infrared optical devices [10]. ZnSe is an extremely stable substance, often manifested as sphalerite structure [11]. Through experiments, scientists have proved that ZnSe has a strong photoelectric effect, so it is believed that ZnSe can replace many toxic materials for industrial production [12].

In recent years, Co has been considered to improve the optical, electrical and magnetic properties of semiconductors due to its special properties as a transition metal. Therefore, the modification of Co by doping has been extensively studied. Adding dopant to semiconductor has become one of the effective methods to improve photocatalytic efficiency [13, 14].

Therefore, in order to improve the catalytic activity and promote the utilization of active components [15], the catalytic efficiency of ZnSe/CoSe on methylene blue solution under different conditions was studied by doping CoSe in ZnSe to study the optimal catalytic efficiency under the optimal conditions.

Experimental

Reagents

Methylene blue (MB) was purchased from Tianjin Guangfu Fine Chemical Research Institute.

*To whom all correspondence should be addressed.

Zinc chloride ($ZnCl_2$) and cobalt chloride ($CoCl_2 \cdot 6H_2O$) were purchased from Shanghai Aladdin Biochemical Technology Co., LTD. Sodium selenite (Na_2SeO_3), ethanolamine (C_2H_7NO) and anhydrous ethanol (C_2H_6O) were purchased from Sinopharm Group Chemical Reagent Co., LTD. Hydrazine hydrate was purchased from Tianjin Bodi Chemical Co. LTD. All reagents were of analytical grade.

Preparation of ZnSe

0.136 g of $ZnCl_2$ and 0.845 g of Na_2SeO_3 were dissolved in 6mL of deionized water, and then 24 mL of ethanolamine and 6 mL of hydrazine hydrate were added slowly during stirring. The mixture was stirred for 45 min until the solution was evenly and fully mixed. The mixed solution was then poured into the Teflon reactor for reaction for 24 h in the air-blown drying oven at 140 ℃. After the reaction, the reactor was naturally cooled down to room temperature. Subsequently, it was washed alternately with anhydrous ethanol and deionized water and then dried for 12 h in a vacuum drying oven at 50 ℃. Finally, the prepared ZnSe was well preserved.

Preparation of ZnSe/CoSe nanocomposite photocatalyst

0.136g $ZnCl_2$, 0.845g Na_2SeO_3 and different proportions of $CoCl_2$ powder were dissolved in 6mL deionized water. 24 mL of ethanolamine and 6 mL of hydrazine hydrate were added during stirring. The mixed solution was then poured into the Teflon reactor for reaction for 24 h in an air-blown drying oven at 140 ℃. After the reaction, the reactor was naturally cooled down to room temperature. Subsequently, it was washed alternately with anhydrous ethanol and deionized water and then dried for 12 h in a vacuum drying oven at 50 ℃. Finally, the prepared nano-catalyst was well preserved.

Photocatalysis experiment

A certain amount of samples were weighed, mixed with MB solutions of different concentrations and volumes, stirred for 40 min under dark conditions, and sampled after reaching adsorption equilibrium. 500 W fluorescent lamp was turned on as the light source, and reaction lasted for 120 min, and sampled six times during the process. The samples were centrifuged and the supernatant was taken at the wavelength of 664 nm to measure the absorbance of the samples. The degradation rate was calculated separately to find out the optimal degradation conditions. The above experiments were repeated with the prepared ZnSe and ZnSe/CoSe, respectively.

Results Analysis and Discussion

Table-1 shows the element distribution represented by EDS of ZnSe/CoSe. As can be seen from Table-1, CoSe was successfully synthesized in ZnSe/CoSe photocatalytic material.

Table-1: EDS of ZnSe/CoSe.

Element	Quality (%)	Atom (%)
Co	2.60	3.17
Zn	42.34	46.61
Se	55.07	50.21

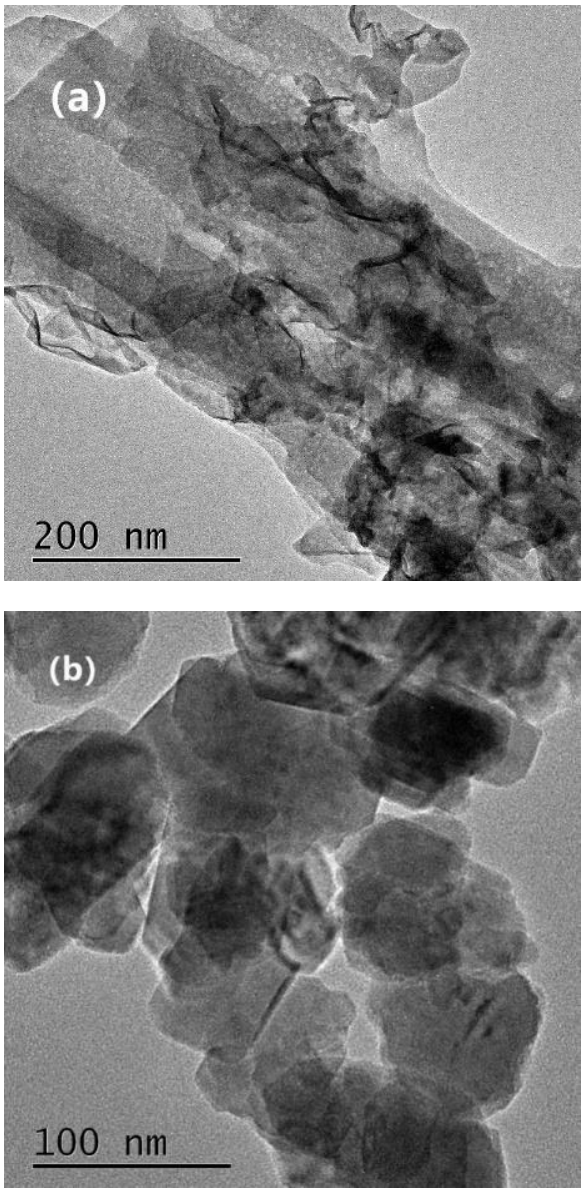

Fig. 1: (a) TEM of ZnSe/CoSe; (b) TEM of ZnSe.

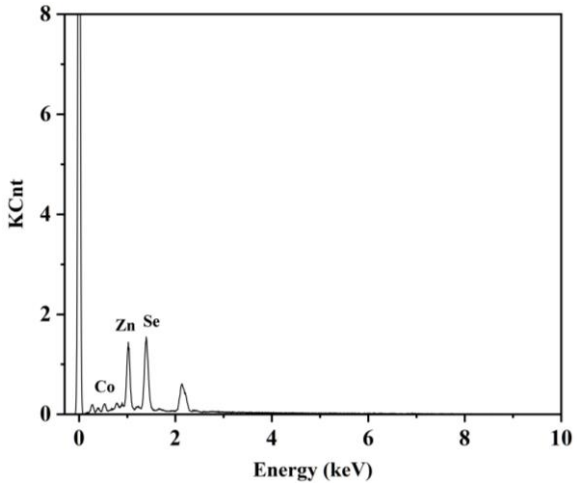

Fig. 2: EDS image of ZnSe/CoSe.

The TEM images of ZnSe/CoSe and ZnSe are shown in Fig. 1 (a) and (b), respectively. As can be seen in Fig. 1(a), the size of the ZnSe/CoSe was about 200 nm and it was composed of many lamellar structures and agglomerates of nanoparticles. As shown in Fig. 1 (b), the ZnSe material obtained had a lamellar structure. Therefore, ZnSe/CoSe had a larger specific surface area, which provided more sites for the attachment of organic substances and was more conducive to the photocatalytic treatment of organic substances.

Fig. 2 shows the EDS image of ZnSe/CoSe. According to the Fig, there were Zn, Se and Co elements in the catalyst sample.

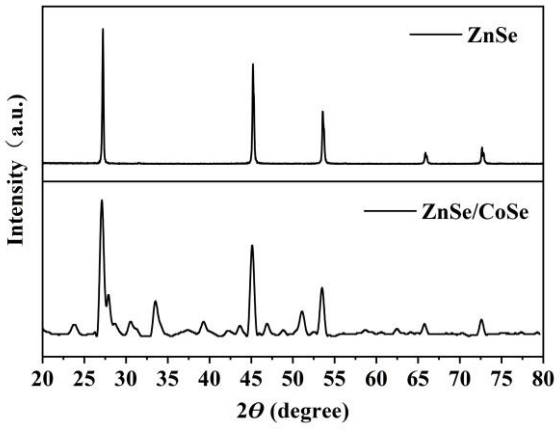

Fig. 3: XRD images of ZnSe and ZnSe/CoSe.

Fig. 3 shows the XRD images of ZnSe/CoSe and ZnSe. As shown in Fig. 3, the peaks were assigned to the diffractions from (111), (220), (311), (400), and (331) planes of the cubic zinc blende phase of ZnSe, respectively, which agrees well with the PDF card (JCPDS file #37-1463). Moreover, no diffraction peaks from Zn or other impurities were observed within the detection limit [16], which indicates that the prepared ZnSe was standard with no impurities.

The diffraction pattern of ZnSe/CoSe nanocomposite photocatalyst is consistent with that of ZnSe, and the diffraction peak of CoSe appeared in the spectrum, indicating the existence of cobalt and selenium.

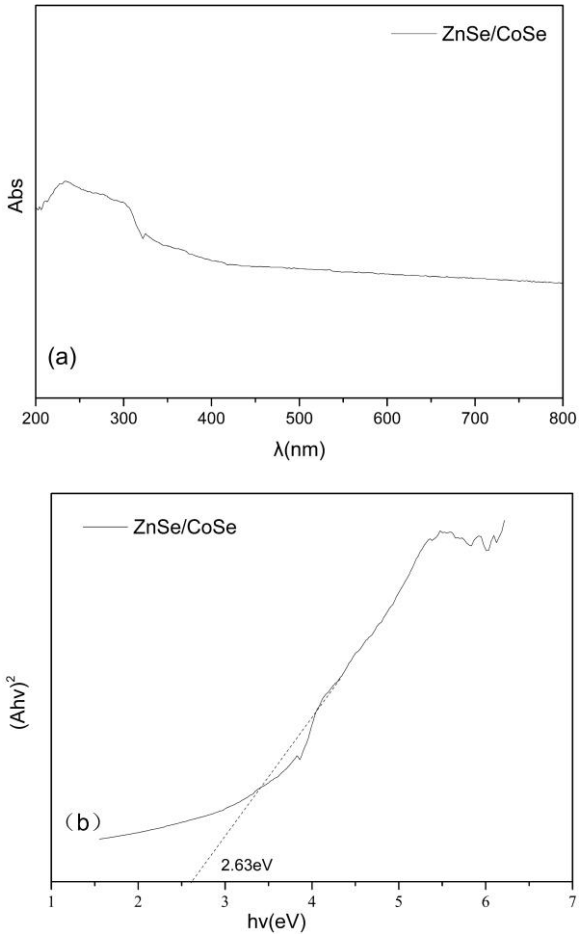

Fig. 4: UV-Vis absorption spectra (a) and estimated band gaps (b) of ZnSe/CoSe.

UV-Vis was performed on ZnSe/CoSe to further study the optical property, as shown in Fig. 4 (a). It can be seen from the Fig that the absorbance band of ZnSe/CoSe was within the range of 200 ~300 nm. Compared with other materials, the absorption band edge redshifted to a longer wavelength [17], indicating that the band gap of ZnSe/CoSe was bigger. The absorption band gap (Eg) can be determined by Eq. (1):

$$(\alpha hv)^2=A(hv-E_g). \quad (1)$$

where $h\nu$ is the photon energy (eV), A is the absorption coefficient, α is a constant, and E_g is the band gap. The band gap can be estimated by extrapolating the linear region in a plot of $(\alpha h\nu)^2$ versus photon energy [18]. As shown in Fig. 4 (b), the band gap energy of ZnSe/CoSe is estimated to be 2.63 eV.

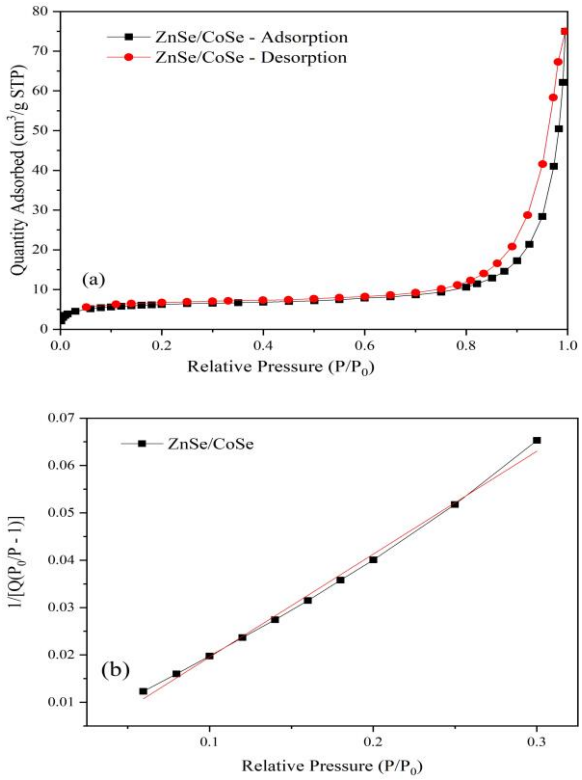

Fig. 5: (a) BET isotherm linear plot of ZnSe/CoSe; (b) BET surface area plot of ZnSe/CoSe.

The BET isotherm linear plot and surface area plot of ZnSe/CoSe are shown in Fig. 5 (a) and (b), respectively. As shown in Fig. 5 (a), the isothermal adsorption of the composite-stripping is of IV type. When P/P_0 = 0~0.5, gentle adsorption quantity increased. When P/P_0 = 0.5~0.8, adsorption increased sharply and the sample size was relatively uniform. When P/P_0 continued to increase, stripping isotherm would not coincide with the adsorption isotherm, instead stripping isotherm was at the top of the adsorption isotherm. Therefore, the material accumulated to form a mesoporous hole.

STP per gram of ZnSe/CoSe paved single molecular layer with an area of 6.87254 m^2. The equation of specific surface area obtained by BET is Eq. (2) and Eq. (3):

$$\frac{S}{m^2/g} = 6.873 \times V_m \qquad (2)$$

$$V_m = \frac{1}{(a+b)} \ldots \qquad (3)$$

It can be seen from Fig. 6 (c) and (d) that the specific surface area of ZnSe/CoSe was1.0004 m^2/g, so it is inferred that ZnSe/CoSe had a large specific surface area and strong photocatalytic effect.

ZnSe/CoSe nanocomposite was further characterized by XPS analysis, as shown in Fig. 6. There were five peaks of Zn, Se, Co, O and C in the samples, and their binding energies were 1024.6 eV, 142.1 eV, 793.6 eV, 531.4 eV and 178.7 eV, respectively. Zn 2p, Se 3d, Co 2p, O 1s and C 1s. XPS results are consistent with EDS results in Fig. 2 [19].

The binding energies obtained in the XPS analyses were calibrated by referring the C 1s peak to 284.6 eV [20]. The Co spectrum showed two major peaks at 779.6 and 793.4 eV (Fig. 6 (b)), which showed a slight shift compared with that of pure cobalt (778.5 eV, 794 eV), which could be assigned to the binding energies of Co $2p_{3/2}$ and Co $2p_{1/2}$, respectively [21]. This confirms the existence of Co^{2+} in the ZnSe/CoSe hybrid catalysts.

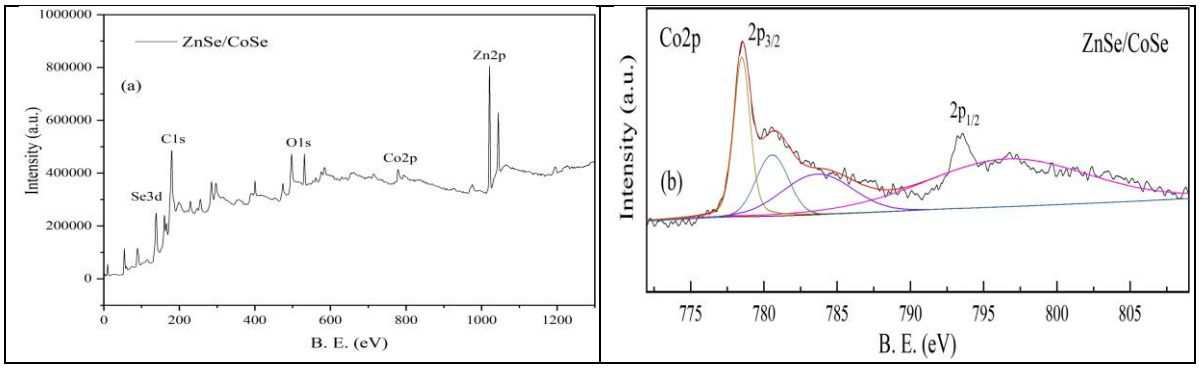

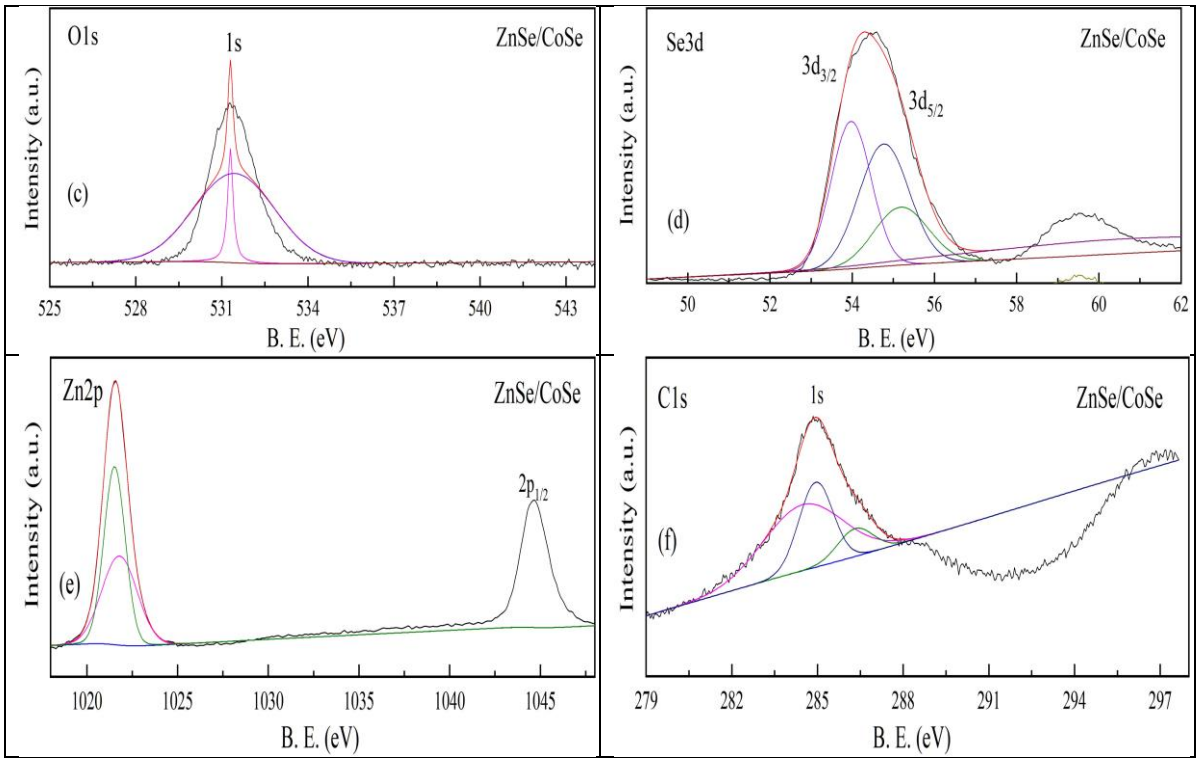

Fig. 6: (a) XPS spectra of ZnSe/CoSe, high-resolution spectrum of ZnSe/CoSe for Co 2 p (b), ZnSe/CoSe for O 1 s (c), ZnSe/CoSe for Se 3 d (d), ZnSe/CoSe for Zn 2 p (e), ZnSe/CoSe for C 1 s (f).

Properties of ZnSe/CoSe nanocomposite

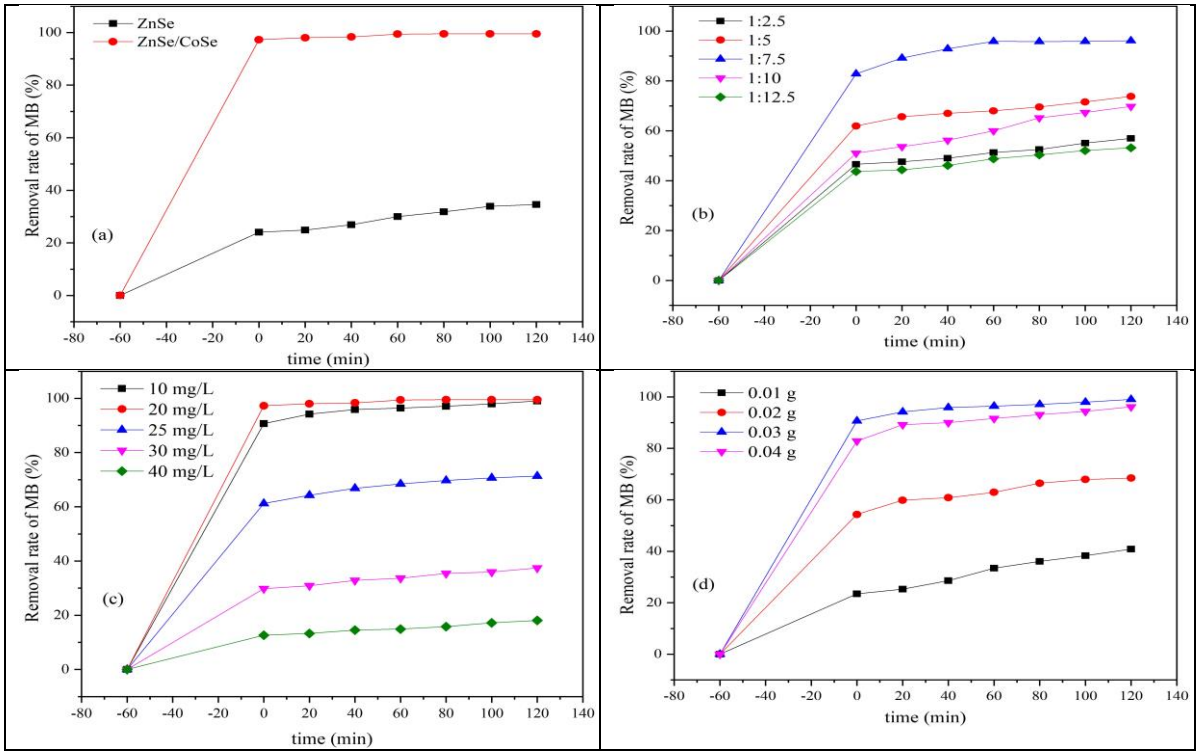

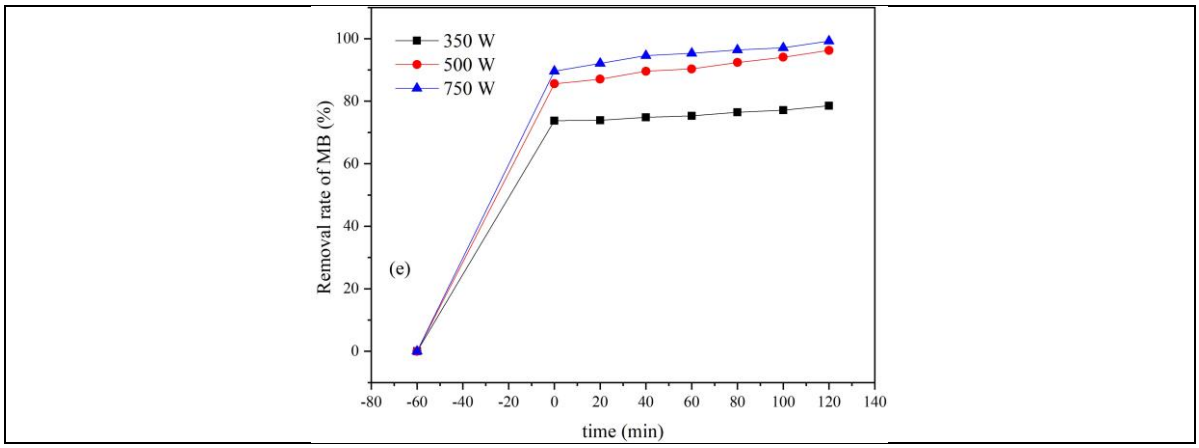

Fig. 7: Under the same condition, the removal effects of ZnSe and ZnSe/CoSe on MB (a). Removal effects of ZnSe/CoSe on MB in different proportions (b). Removal effects of ZnSe/CoSe on MB at different concentrations (c). Removal effects of ZnSe/CoSe on MB under different dosages (d). Removal effects of ZnSe/CoSe on MB under different light intensities (e).

According to Fig. 7 (a), under the same conditions, the degradation rates of ZnSe and ZnSe/CoSe were 28.7% and 99.4 %, respectively. Due to the large specific surface area of composite photocatalysis, the adsorption and photocatalytic effects of doped catalysts were significantly better than those of single catalyst.

Fig. 7 (b) shows that the degradation rate of methylene blue by ZnSe/CoSe increased first and then decreased as the doping ratio of CoSe element increased. When the ratio of Zn: CoSe was 1:2.5, 1:5, 1:7.5, 1:10 and 1:12.5, the degradation rate of methylene blue by the nanocomposite photocatalyst was 53.9 %, 69.7 %, 96.1 %,69.3 % and 55.1 %, respectively. According to the above data, the degradation rate of methylene blue by the nanocomposite photocatalyst was the largest when the ratio of Zn: CoSe was 1:7.5. As the proportion of CoSe increased, the specific surface area of the nanocomposite photocatalyst and the adsorption capacity of methylene blue increased. However, when the optimal doping ratio was reached and the proportion of CoSe continued to increase, the activity and photocatalytic efficiency of ZnSe decreased.

Using the same experimental method, the photocatalytic efficiency under different conditions was successively tested, as shown in Fig. 7(c) (d) and (e). It was found that ZnSe/CoSe photocatalyst with a ratio of 0.03 g Zn/CoSe of 1:7.5 had the highest degradation rate for methylene blue solution of 20 mg/L under the condition of 500 W light intensity.

With the increase of methylene blue concentration and the amount of catalyst added, the specific surface area of the photoreaction of nanocomposite photocatalyst increased, the photocatalytic activity was enhanced, and the photocatalytic efficiency was improved. However, when the photocatalytic efficiency was optimized, the concentration of methylene blue and the dosage of the catalyst continued to increase, and methylene blue dye and catalyst would produce light shading, thus inhibiting the occurrence of light reaction.

As shown in Fig. 7 (e), the photocatalytic efficiency was improved with the increase of light intensity, but since the 750 W light intensity did not significantly improve the photocatalytic efficiency compared with 500 W light intensity. Considering the economic applicability and environmental applicability, 500 W light intensity with a higher cost performance was selected.

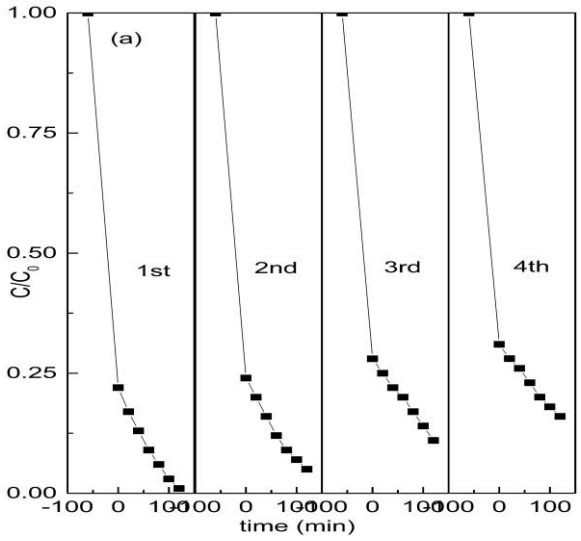

Fig. 8: Recycling tests for ZnSe/CoSe under visible light irradiation.

Table-2: Photocatalytic effect of ZnSe doped with different substances.

Matter	Actor	Catalytic results	References
$CdS/ZnSe/TiO_2$	methyl orange (MO)	The removal of 10 mg/L organics was 90.05% in 120 minutes.	[22]
ZnSe/rGO	MB	The removal of 10 mg/L organics was 96.5% in 120 minutes.	[23]
MWCNT/ZnSe	fuchsine acid	The removal of 10^{-4} mg/L organics was 100% in 50 minutes.	[24]
$ZnO/ZnSe/MoSe_2$	methyl orange (MO)	The removal of 30 mg/L organics was 91.5% in 180 minutes.	[25]
$MoSe_2/ZnSe$	MB	The removal of 2×10^{-5} M organics was 91.5% in 180 minutes.	[26]
$Fe_3O_4/ZnO/ZnSe$	RhB	The removal of 20 mg/L organics was 97.88% in 120 minutes.	[27]
ZnSe/CoSe	MB	The removal of 20 mg/L organics was 99.4% in 120 minutes.	This work

The four cycle experiments were successively conducted on ZnSe/CoSe in the later stage, as shown in Fig. 8. The photocatalytic efficiency of the photocatalyst after the cycle was higher than 80 %, indicating that the photocatalytic activity and stability of the catalyst were good.

Based on the above experiments, we proposed the possible photocatalyst mechanism of ZnSe/CoSe photocatalyst, as shown in Fig. 9. The valence band (VB) of CoSe and ZnSe was 0.08 eV and - 1.26 eV, the conduction band (CB) of CoSe and ZnSe was - 1.7 eV and - 2.9 eV. Therefore, when visible light was irradiated, the photoproduction electronic and holes were formed on the surface of ZnSe/CoSe photocatalyst, and electrons were transferred from CoSe to ZnSe, making ZnSe an electron acceptor. Meanwhile, the electron reacted with O_2 and H_2O on the surface of ZnSe to decompose into -OH, and MB was degraded to other harmless products by free radical redox. CoSe has a stronger ability to absorb visible light and ultraviolet light and a higher photoelectron separation efficiency than other materials, so it inhibits the photoelectron-hole compound and improves the photocatalytic efficiency. Therefore, ZnSe/CoSe photocatalyst has stronger photocatalytic activity in electron transfer and visible light utilization.

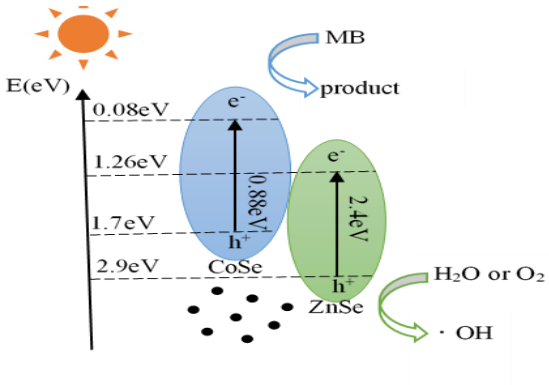

Fig. 9: Proposed photocatalytic mechanism of ZnSe/CoSe.

The degradation results of organic matter by different nano-composite catalysts related to ZnSe are shown in Table 2. For example, 10mg/L of MO could be degraded by 90.05% of $CdS/ZnSe/TiO_2$ in 120 min; 10mg/L of MB could be degraded by 96.5% of ZnSe/rGO in 120 min; 10^{-4} mg/L of fuchsine acid could be degraded by 100% of MWCNT/ZnSe in 50 min.

Conclusions

ZnSe/CoSe was synthesized by hydrothermal method. Through doping modification, the nanocomposite photocatalyst exhibited better band gap and better conductivity than single ZnSe material. At the same time, ZnSe/CoSe demonstrated better conductivity and photocatalytic effect. In addition, the superior photocatalytic effect of ZnSe/CoSe was discussed, which provides a new theoretical and experimental basis for the research and development of nanocomposite photocatalysts in the future.

Acknowledgements

This work was supported by Shandong Province Natural Science Foundation (ZR2017MB049).

Declaration of Interest Statement

The authors declare that they have no conflict of interest.

References

1. T. N. J. I. Edison, R. Atchudan, M. G. Sethuraman and Y. R. Lee. Reductive-degradation of carcinogenic azo dyes using Anacardium occidentale testa derived silver nanoparticles, *J. Photochem. Photobiol. B: Biol.*, **162**, 604 (2016).

2. P. Singh, G. Kaur, K. Singh, B. Singh, M. Kaur, M. Kaur, U. Krishnan, M. Kumar, R. Bala and A. Kumar. Specially designed B_4C/SnO_2 nanocomposite for photocatalysis: traditional ceramic with unique properties, *Appl. Nanosci*., **8**, 1 (2018).
3. M. K. Singha and A. Patra. Highly efficient and Reusable ZnO microflower photocatalyst on stainless steel mesh under UV–Vis and natural sunlight, *Opt. Mater.*, **107**, 110000 (2020).
4. X. Yue, S. Jiang, L. Ni, R. Wang, S. Qiu and Z. Zhang. The highly efficient photocatalysts of Co/TiO_2: Photogenerated charge-transfer properties and their applications in photocatalysis, *Chem. Phys. Lett.*, **615**, 111 (2014).
5. S. Li, L. Wang, X. Su, Y. Pan, D. Gao and X. Han. Optical properties of Co-doped ZnSe thin films synthesized by pulsed laser deposition, *Thin Solid Films*, **692**, 137599 (2019).
6. K. Feng, W. Xue, X. Hu, J. Fan and E. Liu. Z-scheme CdSe/ZnSe heterojunction for efficient photocatalytic hydrogen evolution, *Colloids Surf. Physicochem. Eng. Aspects*, **622**, 126633 (2021).
7. F. Mirnajafizadeh, D. Ramsey, S. McAlpine, F. Wang, P. Reece and J. A. Stride. Hydrothermal synthesis of highly luminescent blue-emitting ZnSe (S) quantum dots exhibiting low toxicity, *Mater. Sci. Eng., C*, **64**, 167 (2016).
8. E. Oksenberg, R. Popovitz-Biro, K. Rechav and E. Joselevich. Guided Growth of Horizontal ZnSe Nanowires and their Integration into High-Performance Blue–UV Photodetectors, *Adv. Mater.*, **27**, 3999 (2015).
9. M. Kamruzzaman and J. A. Zapien. Synthesis and characterization of ZnO/ZnSe NWs/PbS QDs solar cell, *J. Nanopart. Res.,* **19**, 125 (2017).
10. M. Vinita, S. W. James and M. Ganapathy Senthil. High-contrast GeTe4 waveguides for mid-infrared biomedical sensing applications, *Proc.SPIE*, **8988**, (2014).
11. L. Deng, G. Feng, S. Dai, H. Zhang and S. Ning. The phase transition and optical properties of Cr^{2+} doped ZnSe under high pressure, *Results Phys.*, **12**, 776 (2019).
12. M. Makhavikou, F. Komarov, I. Parkhomenko, L. Vlasukova, O. Milchanin, J. Żuk, E. Wendler, I. Romanov, O. Korolik and A. Togambayeva. Reprint of "Structure and optical properties of SiO_2 films with ZnSe nanocrystals formed by ion implantation", *Surf. Coat. Technol.,* **355**, 328 (2018).
13. N. P. F. Gonçalves, M. C. Paganini, P. Armillotta, E. Cerrato and P. Calza. The effect of cobalt doping on the efficiency of semiconductor oxides in the photocatalytic water remediation, *J. Environ. Chem. Eng*., **7**, 103475 (2019).
14. J. Yin and X. Zhang. The Investigation of Sn heavily doped ZnSe for promising intermediate band materials, *J. Phys. Chem. Solids*, **152**, 109951 (2021).
15. J. Chen, Y. Gao, Y. Fu and S. Pan. Ag Nanoparticles Decorated N-Doped Carbon Black as a High-Performance Catalyst for Catalytic Hydrogenation of p-Nitrophenol, *Nano*, **14**, 1950095 (2019).
16. B. Feng, J. Cao, J. Yang, S. Yang and D. Han. Characterization and photocatalytic activity of ZnSe nanoparticles synthesized by a facile solvothermal method, and the effects of different solvents on these properties, *Mater. Res. Bull*., **60**, 794 (2014).
17. H. Liu, Y. Hu, X. He, H. Jia, X. Liu and B. Xu. In-situ anion exchange fabrication of porous ZnO/ZnSe heterostructural microspheres with enhanced visible light photocatalytic activity, *J. Alloys Compd.*, **650**, 633 (2015).
18. J. Huang, H. Ren, K. Chen and J.-J. Shim. Controlled synthesis of porous Co_3O_4 micro/nanostructures and their photocatalysis property, *Superlattices Microstruct.*, **75**, 843 (2014).
19. C. Yang, X. Wang, Y. Ji, T. Ma, F. Zhang, Y. Wang, M. Ci, D. Chen, A. Jiang and W. Wang. Photocatalytic degradation of methylene blue with ZnO@C nanocomposites: Kinetics, mechanism, and the inhibition effect on monoamine oxidase A and B, *NanoImpact*, **15**, 100174 (2019).
20. X. Shi, S. Quan, L. Yang, G. Shi and F. Shi. Facile synthesis of magnetic Co_3O_4/BFO nanocomposite for effective reduction of nitrophenol isomers, *Chemosphere*, **219**, 914 (2019).
21. X. Xu, Y. Ge, M. Wang, Z. Zhang, P. Dong, R. Baines, M. Ye and J. Shen. Cobalt-Doped $FeSe_2$-RGO as Highly Active and Stable Electrocatalysts for Hydrogen Evolution Reactions, *ACS Appl. Mater. Inter*., **8**, 18036 (2016).
22. V. Nguyen, W. Li, V. Pham, L. Wang, P. Sheng, Q. Cai and C. Grimes. A $CdS/ZnSe/TiO_2$ nanotube array and its visible light photocatalytic activities, *J. Colloid Interface Sci.*, **462**, 389 (2016).
23. R. Yousefi, H. R. Azimi, M. R. Mahmoudian and W. J. Basirun. The effect of defect emissions on enhancement photocatalytic performance of ZnSe QDs and ZnSe/rGO nanocomposites, *Appl. Surf. Sci*., **435**, 886 (2018).

24. H. Wu, Q. Wang, Y. Yao, C. Qian, P. Cao, X. Zhang and X. Wei. Microwave-assisted synthesis and highly photocatalytic activity of MWCNT/ZnSe heterostructures, *Mater. Chem. Phys*., **113**, 539 (2009).
25. Y. Yang, Z. Wu, R. Yang, Y. Li, X. Liu, L. Zhang and B. Yu. Insights into the mechanism of enhanced photocatalytic dye degradation and antibacterial activity over ternary ZnO/ZnSe/$MoSe_2$ photocatalysts under visible light irradiation, *Appl. Surf. Sci*., **539**, 148220 (2021).
26. P. Tian, T. Tang, J. Zhang, S. Lin, G. Huang, J. Zeng, Z. Kong, H. Wang, J. Xi and Z. Ji. High photocatalytic and photoelectrochemical performance of a novel 0D/2D heterojunction photocatalyst constructed by ZnSe nanoparticles and $MoSe_2$ nanoflowers, *Ceram. Int.*, **46**, 13651 (2020).
27. G. Xu, Z. Zhang, T. Li, M. Du, Y. Guan and C. Guo. Continuous high-efficient degradation of organic pollutants based on sea urchin-like Fe_3O_4/ZnO/ZnSe heterostructures in photocatalytic magnetically fixed bed reactor, *Colloids Surf. Physicochem. Eng. Aspects*, **603**, 125198 (2020).